J Mater Sci (2015) 50:1605–1612
DOI 10.1007/s10853-014-8721-2

Flammability and tensile properties of polylactide nanocomposites with short carbon fibers

Kuo-Chung Cheng · Yan-Huei Lin · Wenjeng Guo · Tsu-Hwang Chuang · Shun-Chih Chang · Sea-Fue Wang · Trong-Ming Don

Received: 19 August 2014 / Accepted: 11 November 2014 / Published online: 20 November 2014

Abstract Nanocomposites of polylactide (PLA) with aluminum hydroxide (ATH), short carbon fibers (CF), and montmorillonite (MMT) were prepared via direct melt blending. The exfoliated and intercalated clay structures with some aggregations in the PLA matrix were observed. The tensile strength and elongation at break of the PLA composite caused by the high content of the retardant ATH were improved by adding modified MMT and CF to replace a portion of ATH in the PLA matrix. The thermal degradation temperatures and char residue of the PLA/ATH/MMT/CF nanocomposites as determined by thermogravimetric analysis were higher than without MMT. Furthermore, a novel method was proposed to analyze the flammability of composite using an infrared camera, which could capture the apparent thermal image of the sample during UL 94 V test. It was found that, with addition of the MMT and short CF, a more effective insulation layer could be formed on the ablating surface of the PLA/ATH composite, and the high thermal conductivity of the CF might increase the release rate of heat from the surface composite during burn, thus the PLA/ATH/MMT nanocomposite containing short carbon fibers having a V-0 rating without flaming dripping could be obtained.

Electronic supplementary material The online version of this article (doi:10.1007/s10853-014-8721-2) contains supplementary material, which is available to authorized users.

K.-C. Cheng (✉) · Y.-H. Lin · W. Guo · T.-H. Chuang · S.-C. Chang
Department of Chemical Engineering and Biotechnology, National Taipei University of Technology, Taipei 10608, Taiwan
e-mail: gordon@ntut.edu.tw

S.-F. Wang
Department of Materials and Mineral Resources Engineering, National Taipei University of Technology, Taipei 10608, Taiwan

T.-M. Don
Department of Chemical and Materials Engineering, Tamkang University, Tamsui District, New Taipei City 25137, Taiwan

Introduction

Polylactide (PLA) is a biodegradable thermoplastic polymer and one of the most promising and important biodegradable polymer. PLA can be produced from renewable resources, such as starch, with relatively low cost and large production volume [1–8]. Therefore, PLA has found widespread use in biomedical materials, packaging, bags, films, and fibers. However, PLA is highly combustible, which limits its use as an electronic or electrical material. Furthermore, the dripping of flaming polymer may cause injury to human skin directly and could promote the progression of the fire. Several researchers have reported blending conventional or novel intumescent flame retardants with PLA to improve its flame retardation and anti-dripping performance when burning [9, 10].

Incorporating low loads of nanoscale fillers into polymer composites has been extensively studied to not only improve their mechanical properties and gas barrier performance but also reduce their flammability [11–15]. Polymer/layered silicate (PLS) nanocomposites have attracted great interest due to the low cost and the amenability of clays to a variety of manufacturing processes. Polymer/clay nanocomposites not containing additional flame retardants exhibited a lower heat release rate (HRR) and peak HRR than the neat polymers during combustion in a cone calorimeter [16, 17]. During this combustion, the clay in the polymer matrix collapsed to form a clay-rich barrier, which slowed but did not extinguish the burning; therefore, the total heat release could not be reduced. Thus, adding other flame retardants, such as aluminum trihydrate (ATH) or aluminum hypophosphite

(AHP), to the PLS nanocomposite is an attractive means for increasing its thermal stability and flame retardant properties. For example, adding nanodispersed layered silicate and ATH flame retardants to an EVA/LLDPE blend produces a synergistic flame retardant effect and smoke-suppressing ability in the composite [18]. PLA-based nanocomposites can be prepared using two different nanofillers, expanded graphite and organically modified montmorillonite, via melt compounding [4]. The thermal and mechanical properties of PLA were improved in the presence of both nanoparticles, which were attributed to the good dispersion and the co-reinforcement effect. In our previous study, PLA nanocomposites containing ATH and modified montmorillonite (MMT) were prepared via direct melt compounding. Exfoliated and intercalated clay structures were observed in the matrix. The V-0 rating (UL 94 V) was achieved for the PLA nanocomposite. Nevertheless, the high flame retardant ATH loading resulted in the lower tensile strength and elongation at break [19].

Carbon fibers (CF) are conventionally used to reinforce polymer-based composites due to its high mechanical strength, modulus, and outstanding thermal properties. Carbon fiber reinforced PLA composites were fabricated via solvent blending and solvent impregnation processes, and the mechanical properties were improved upon the addition of the carbon fiber [20, 21]. Furthermore, short carbon fiber-filled polymer composites can be easily prepared via extrusion compounding and injection molding [22, 23]. Therefore, in this study, short carbon fibers were added to replace some ATH filler in the PLA/ATH/MMT composite to improve the mechanical properties of the PLA nanocomposites. Polylactide composites containing ATH, MMT (Cloisite 30B), and short CF were prepared via direct melt compounding in a Brabender. The morphology, thermal degradation, and mechanical properties of the PLA/ATH/MMT composites were investigated by SEM, XRD, TEM, TGA, and tensile testing. The flame retardant properties were further analyzed via a vertical burning UL94 test and cone calorimetry. The surface thermal image of the sample during UL 94 V test was further captured by an infrared camera. It could help us to understand the flame retardant properties of the different samples. The thermal and mechanical properties, flammability, and dripping resistant of the nanocomposites upon the addition of the short CF will be discussed.

Experimental

Materials

PLA (PLA2002D™) was purchased from Nature-Works LLC. Aluminum trihydrate (ATH, H-42 M grade) with an average particle size of approximately 1.1 μm was obtained from Showa Denko Co. Ltd., Japan. Modified montmorillonite clay containing methyl tallow bis(2-hydroxyethyl) ammonium (Cloisite 30B) and carbon fiber (CF, TC-3512 K, diameter of 7 μm) was purchased from Southern Clay Products Inc. and Tairyfil (Taiwan), respectively. CF with no surface treatments was cute into short lengths of approximately 1–2 cm before compounding.

Sample preparation

The PLA, ATH, Cloisite 30B, and short CF were dried overnight at 90 °C under vacuum before compounding. PLA, ATH, MMT, and carbon fibers were melt compounded in a Brabender (PLE-331, ATLAS) at 50 rpm for 6 min at 160 °C. The formulations of the PLA composites are listed in Table 1.

Analysis

X-ray diffraction spectra (XRD) were obtained using a diffractometer (PANalytical X'Pert PRO) with Cu radiation ($\lambda = 0.154$ nm). The composite morphology of the PLA/ATH/MMT containing the short fiber was sputter coated with gold and examined with a scanning electron microscope (SEM, Hitachi S-3000H). The clay morphology in the composite was also observed with either a JEOL transmission electron microscope at 200 kV (model JEM2010) or SEM. The thermal degradation of the PLA composite sample, approximately 10 mg, was measured using a thermogravimetric analyzer (TGA, TA Q-50) under flowing air (90 mL/min) at a heating rate of 20 °C/min.

Table 1 The formulations of the PLA nanocomposites (wt%)

Sample	PLA	ATH	MMT	CF
PLA	100	0	0	0
ATH	0	100	0	0
Cloisite 30B	0	0	100	0
F20	60	20	0	20
F19	60	20	1	19
F18	60	20	2	18
F17	60	20	3	17
F16	60	20	4	16
F15	60	20	5	15
B40	60	40	0	0
B39	60	39	1	0
B38	60	38	2	0
B37	60	37	3	0
B36	60	36	4	0
B35	60	35	5	0

The limiting oxygen indices (LOI) of the PLA composites were determined using a Suga test apparatus (model: ON-1). A cone calorimeter (Atlas Cone 2) was used to investigate the composite flammability (size: 100 mm × 100 mm × 6 mm) at an incident heat flux of 50 kWm^{-2}. The UL94 vertical test was performed according to the ASTM D3801 testing procedure (sample size: 120 mm × 13 mm × 3 mm). The thermal image on the surface of sample during test was further recorded using an infrared camera (TAS, Ching Hsing). The mechanical tensile properties of the PLA composites (type IV specimen shape and dimensions of ASTM D638) were measured using a tensile tester (Tensometer 10, Monsanto Co., at an extension rate of 5 mm/min at room temperature.

Results and discussion

Morphology

The distance between silicate layers can be observed from the basal reflection of the X-ray diffraction curve [24]. In our previous work, it was found that adding ATH might facilitate the melt intercalation of PLA into the organically modified MMT during compounding [19]. The structure of the PLA/ATH/MMT nanocomposite was exfoliated and intercalated as observed by XRD and TEM. The modified clay, Cloisite 30B, exhibits a diffraction peak at approximately 5.3° corresponding to the basal reflection (001) and a d-spacing of approximately 1.7 nm. As shown in Fig. 1, there was no apparent peak in the XRD plot of the samples F15-19. The noisy X-ray signal might be caused by the fillers, and the dispersion of the MMT in PLA could not be confirmed by the XRD plot.

The morphology of the PLA/ATH/MMT nanocomposite containing short CF was further observed using TEM. As shown in Fig. 2a, the larger dark image indicates the crushed ATH particles or the agglomerations of MMT after melt compounding, and the light gray image implies some MMT sheets could be well dispersed in the PLA matrix [24]. The high-magnification TEM image of sample F15 showed several intercalated tactoids composed of a number of lamellae and individual MMT sheets as observed in Fig. 2b. Furthermore, Fig. 3 shows the surface morphology of the PLA/ATH/MMT composite containing short CF, sample F15, after etching and rinsing with THF. It was found that the carbon fiber length was reduced to 208 ± 69 μm after compounding. The ATH particles and MMT were coagulated with the short CF after treatment with THF. Therefore, it is hard to distinguish MMT from ATH by the SEM picture.

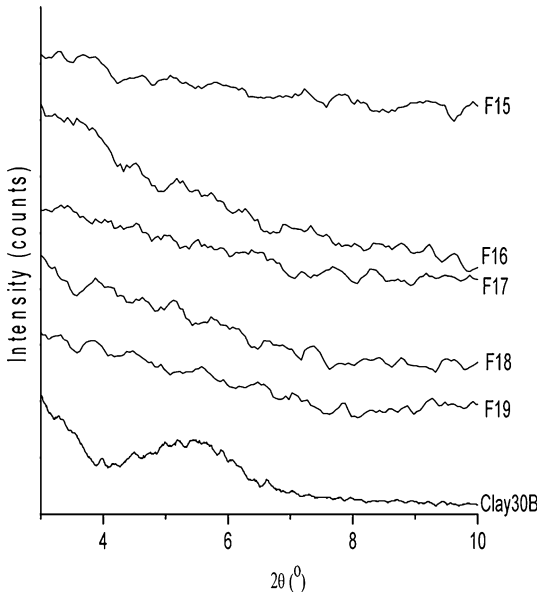

Fig. 1 XRD of the PLA/ATH/MMT/CF nanocomposites

Thermal degradation

The thermal properties of the PLA composites were investigated via TGA in air as shown in Fig. 4. Table 2 indicates the thermal degradation of the composites as determined by TGA. The temperatures of 5 % loss (T_d) and the maximum thermal degradation rate (T_{max}) of ATH were approximately 250 and 281 °C, respectively. The main thermal decomposition of the unmodified PLA occurred at approximately 371 °C and was reduced to approximately 320 °C upon the addition of 40 wt% ATH (sample B40) [19]. This drop was due to the reduced dehydration temperature of the ATH filler. Adding 20 wt% of the CF to replace a portion of the ATH, sample F20, yielded a T_d of 282 °C, which is very close to that of sample B40 without any CF; however, the T_{max} is lower, approximately 312 °C. Adding MMT to the composites could increase the degradation temperature up to approximately 350 °C for the sample F15 with 5 % of MMT and 15 % CF, for example. A barrier layer could be formed by the incorporation of clay sheets, and a decrease in oxygen and volatile degradation products permeability or diffusivity throughout the barrier caused the shift of the degradation temperature [24, 25]. Therefore, incorporating layered silicates into the PLA/ATH/CF composites could further increase thermal stabilization during degradation. Moreover, it was found that both the values of T_{max} and char residue of the PLA nanocomposites with CF, MMT, and 20 % of ATH, samples F15-F19, were higher than those of the relative composites without any CF, samples B35-B39. It has possibly resulted from the high thermal conductivity of the carbon

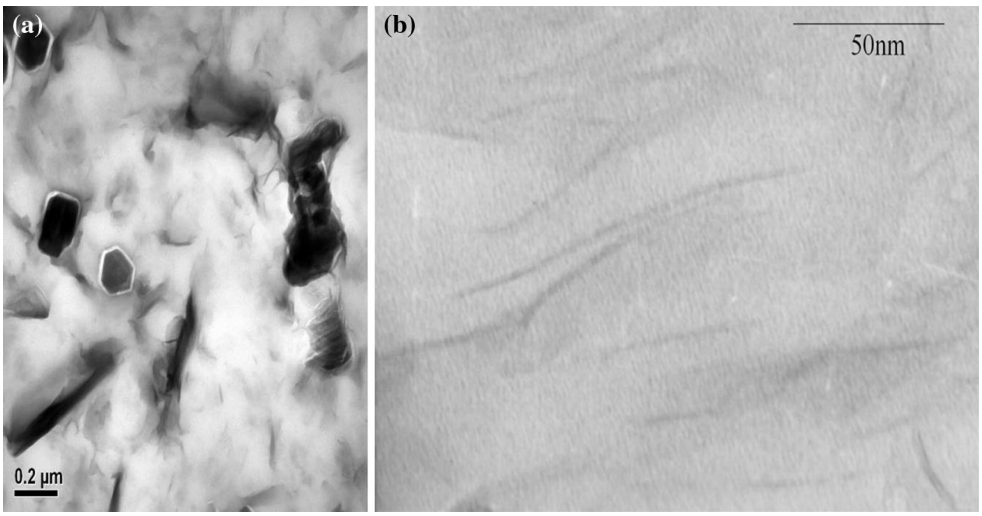

Fig. 2 TEM of the PLA/ATH/MMT/CF nanocomposite (sample F15, PLA/ATH/MMT/CF ratio of 60:20:5:15)

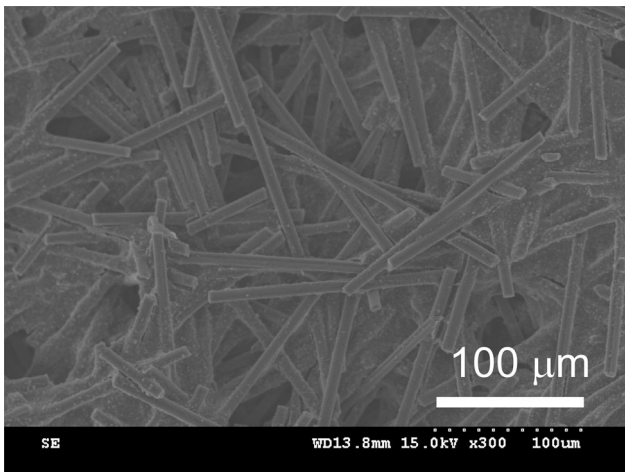

Fig. 3 SEM of the PLA/ATH/MMT/CF nanocomposite surfaces (sample F15)

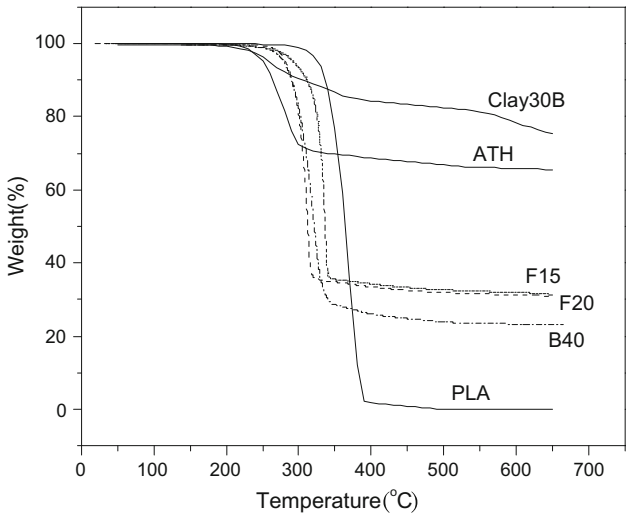

Fig. 4 Weight loss curves for PLA, ATH, modified MMT, and the PLA composites

fibers which help in releasing the thermal energy from the surface layer [26, 27].

Flammability properties

The limiting oxygen index (LOI) of PLA and its composites with ATH, Cloisite 30B, or CF are given in Table 3. The LOI of neat PLA is 20.5 %. This value increased to 30 % upon the addition of 40 % of ATH (sample B40). Replacing some of the ATH in the PLA composites with layered silicates, samples B36-B39, resulted in an LOI similar to the initial value. The layered clay in the burning nanocomposite was unable to integrate with ATH to form a more rigid insulation layer on the ablating surface and possibly dripped away with the melting material; thus, adding MMT does not improve the LOI of the PLA composites [19]. Replacing a portion of the ATH in the PLA nanocomposite with 15 % of CF, sample F15, increased the LOI to approximately 32 %. The result was consistent with the finding of the TGA test. It implies that addition of CF with the high thermal conductivity could increase the heat dissipation rate from the burning sample, and might improve the flame retardant property of the PLA nanocomposite [26].

The cone calorimeter is a useful bench-scale tool for studying the flammability and HRR during burning for a material. The peak HRR and heat flux of the neat PLA were approximately 629 and 259 kWm^{-2}, respectively, as shown in Fig. 5 and Table 4. These results indicate conventional ATH retardants significantly affect the PLA composite. For composites containing 40 wt% ATH (B40), the peak and average HRRs were reduced to approximately 412 and

Table 2 Thermal degradation properties of PLA/ATH/MMT composites

Sample	T_d (°C)[a]	T_{max} (°C)[b]	Char residue at 650 °C (wt%)
PLA	326.6	371.2	0.09
ATH	250.4	280.5	65.6
Cloisite 30B	259.2	261.5	75.3
F20	281.7	312.0	30.5
F19	292.3	326.5	32.1
F18	299.6	328.4	32.0
F17	305.1	334.0	33.2
F16	295.8	336.5	30.9
F15	295.5	350.4	34.4
B40	279.3	321.4	23.2
B39	282.5	318.5	21.8
B38	285.3	319.9	25.1
B37	288.7	322.7	21.8
B36	289.3	332.7	25.5
B35	288.0	337.3	25.7

[a] The temperature at 5 % weight loss under air purge and a heating rate of 20 °C/min

[b] The temperature at the maximum thermal decomposition rate

Table 3 Flame retardant properties of the PLA composites

Sample	LOI (%)	UL-94	Total flaming combustion of all five specimens (sec)	Flame dripping	Cotton ignited
PLA	20.5	Fail	>250[a]	Yes	Yes
F20	29.0	V-2	60	Yes	Yes
F19	29.0	Fail	>250	No	No
F18	28.5	Fail	>250	No	No
F17	28.5	V-1	54	No	No
F16	30.0	V-0	26	No	No
F15	32.0	V-0	22	No	No
B40	30.0	V-0	11	Yes	No
B39	30.5	V-0	16	Yes	No
B38	31.0	V-2	155	Yes	Yes
B37	30.0	V-2	162	Yes	Yes
B36	30.0	V-2	107	Yes	Yes
B35	30.0	Fail	>250	Yes	Yes

Fail no rating of UL-94 tests

[a] The flame on PLA sample might drop away from the specimen during test

117 kWm^{-2}, respectively. Adding the short carbon fiber to the PLA/ATH/MMT composite as a substitutive filler could further reduce the average HRR. Furthermore, Fig. 6 shows the char remaining of the sample on an aluminum foil after burning in the cone calorimeter. The unfilled PLA was

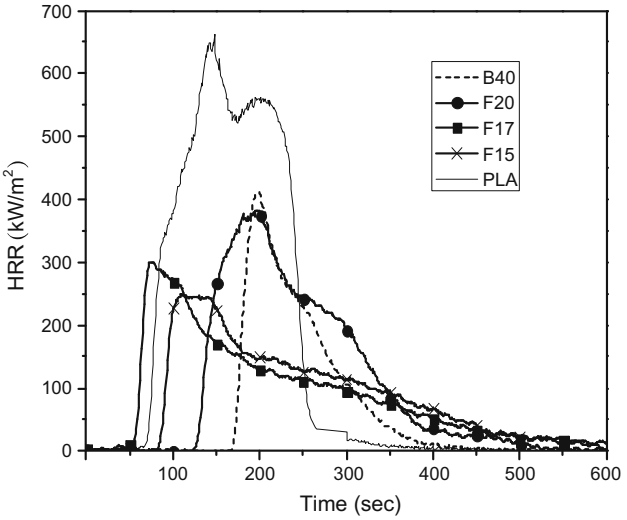

Fig. 5 Heat release rate curves of PLA and its composites

Table 4 Flammability properties of PLA composites determined by the cone calorimeter

Sample	Time to ignition (sec)	Peak HRR (kW m^{-2})	Av. HRR (kW m^{-2})
PLA	58.0	628.5	259.2
F20	48.4	374.3	96.2
F17	60.3	310.6	91.3
F15	53.8	262.4	91.6
B40	142.0	411.8	117.4
B38	62.0	246.3	102.0
B35	65.0	252.0	121.6

almost burned out completely after the test. With addition of 20 % of ATH and 20 % of CF, sample F20, the char with porous structure was formed. Once the MMT was added, for samples F17 or F15, the char became denser than that of F20. The results are very consistent with the TGA and cone calorimetry tests, and imply a more effective insulation layer could be formed on the ablating surface of the nanocomposite during cone test.

The UL 94 V flammability rating results and the thermal images captured by the IR camera for vertical burns are shown in Table 3 and Figure A1 (Supplementary Material), respectively. Although the IR image was affected by the flame, soot, and the IR transparent properties of the composite, it could still provide some important information from the apparent thermal profile. The unfilled PLA was highly flammable. After removal of the burner ignition, the PLA sample continued to burn for a long time, and the cotton indicator was ignited by the melt drips. Sometimes, the flame on the end of sample was wholly taken away by a melt dripping; then the fire on sample was extinguished.

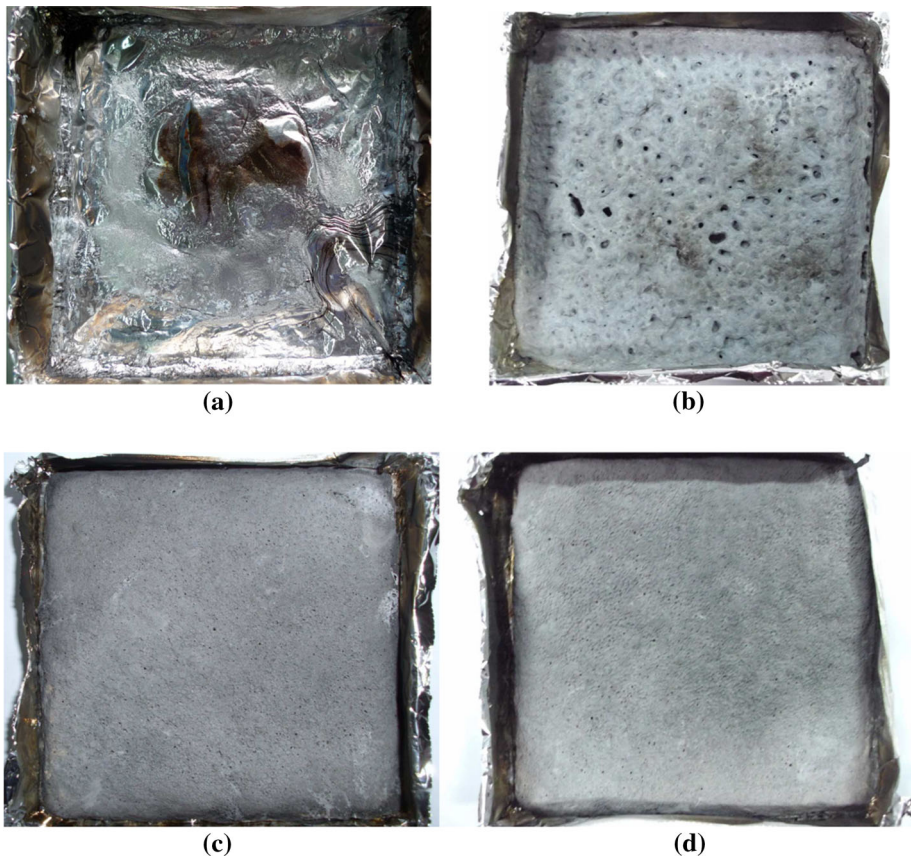

Fig. 6 Chars of **a** PLA, and PLA/ATH/MMT/CF nanocomposites **b** sample F20; **c** F17; and **d** F15 after the cone calorimetry test

Figure 7a shows the thermal images of the samples while the ignition burner had been moved away from the sample for one second. The apparent temperature profiles along the vertical center line of the sample were determined by the thermal images, and the profiles dependent on the vertical distance from the bottom, h, of sample are plotted in Fig. 7b. First, the surface temperature of the PLA sample decreased from 350 °C to about 260 °C at $h = 5$ mm and then increased again to a peak of 300 °C around 10 mm, which could be resulted from the heat of flame. After that, the temperature further decreased gradually along the height, h. Note that, at $h = 30$ mm, the temperature was still higher than the melting point of PLA, about 160 °C. It could result in the melt dripping as shown in the Figure A1.

Once the PLA was combined with 40 % ATH (B40), the burning stopped sooner and the cotton indicator ignition was avoided. Therefore, the classification was upgraded to a V-0 rating [19]. The temperature on the bottom of the sample decreased to about 220 °C due to the dehydration of the ATH filler. Around $h = 5$ mm, the temperature declined rapidly to 110 °C. It implied that there was a high thermal barrier formed by the ablating layer. When 40 % of ATH in the sample B40 was partially replaced by 20 % CF, the high thermal conductivity of the CF might increase the heat dissipation rate from the sample F20 during the cone test, which resulted in the lower HRR compared to the sample B40. However, an effective rigid barrier layer could not be formed on the ablating surface of the sample F20, the LOI value was low (approximately 30 %), and the melt dripping ignited the cotton under the UL 94 V test. The sample was given a V-2 rating.

Because the high thermal conductivity of the CF could increase the dissipation rate of heat from the skin layer, and the incorporation of MMT sheets could further form the effective rigid layer as mentioned above, the flame dripping could be avoided with addition of the substitutive filler Cloisite 30B [25, 26]. When 4 or 5 wt% of the filler Cloisite 30B was added, that was samples F16 or F15, it not only stopped the flame dripping but also improved the classification to V-0. Furthermore, a sharp decline in the surface temperature profile of sample F15 is observed in Fig. 7b, and the temperature could be reduced quickly to be lower than 150 °C at $h = 10$ mm. Therefore, the fire could be extinguished quickly, and the melt dripping could also be prevented.

Mechanical properties

The unmodified PLA has a tensile modulus of 3.7 GPa, a tensile strength of 55.2 MPa, and an elongation at break of

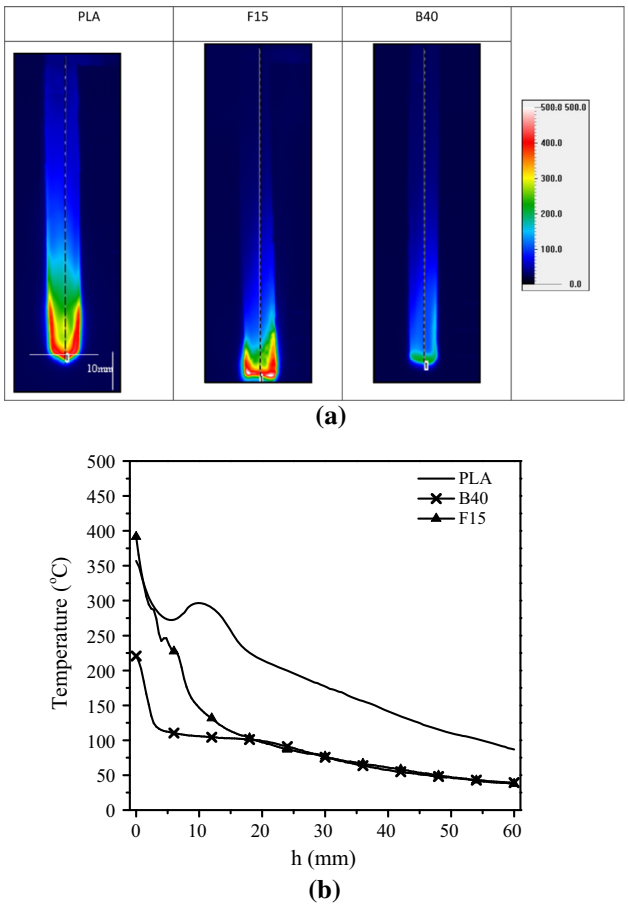

Fig. 7 Surface temperature profiles dependent on the distance from the bottom of the sample

10 % as shown in Table 5. The tensile moduli for most of these composites increased after adding ATH. However, the composites lost mechanical tensile strength and became brittle at higher ATH loadings. The mechanical properties of the PLA/ATH composite were found to improve when MMT Cloisite 30B replaced a portion of the filler for a certain composition. Adding 3 % MMT increased the tensile modulus and tensile strength of composite B37 to 5 GPa and 52.4 MPa, respectively, which is a 17 % increase relative to the sample without MMT, sample B40 [19]. Both the tensile strength and elongation at break of the PLA composite increased by further substituting a portion of the ATH with CF. For example, the tensile strength and elongation at break of sample F20, which contained 20 % CF and 20 % ATH, increased to approximately 84 MPa and 7.6 %, respectively, which are higher than that without any CF, sample B40 (45 MPa and 5.8 %). However, adding the MMT to replace a part of CF in the composite decreased the tensile strength, and it denoted that the reinforcement effect of the short CF was better than MMT for the PLA composite.

Table 5 Mechanical properties of PLA composites

Sample	Tensile modulus (GPa)	Tensile strength (MPa)	Elongation at break (%)
PLA	3.69 (±0.05)	55.2 (±3.07)	9.98 (±0.52)
F20	4.88 (±0.28)	83.6 (±17.3)	7.59 (±0.98)
F19	5.87 (±0.48)	86.7 (±4.45)	6.98 (±0.10)
F18	6.62 (±0.31)	79.1 (±7.03)	6.93 (±0.28)
F17	4.42 (±1.02)	77.2 (±4.81)	7.49 (±0.68)
F16	4.66 (±1.04)	63.0 (±13.8)	5.96 (±0.59)
F15	4.51 (±0.40)	64.5 (±7.37)	6.77 (±0.30)
B40	4.51 (±0.38)	44.9 (±0.67)	5.78 (±0.30)
B39	4.65 (±0.50)	47.4 (±2.59)	5.67 (±0.42)
B38	5.02 (±0.37)	44.4 (±3.61)	5.24 (±0.12)
B37	5.01 (±0.05)	52.4 (±1.29)	5.81 (±0.25)
B36	5.50 (±0.09)	44.6 (±5.45)	4.49 (±0.43)
B35	4.99 (±0.25)	43.8 (±1.97)	4.63 (±0.25)

The tensile modulus of the PLA/ATH/CF composite increased with the addition of the MMT at a low content and reached a peak value of 6.6 GPa for the sample F18 with 2 % MMT. A high MMT content might lead to agglomeration of some MMT sheets, which could reduce the mechanical tensile strength or modulus. Moreover, it was reported that the filler, such as MMT, would change the crystal structure and the degree of crystallinity of the PLA matrix, which played an important role in the mechanical properties [28]. We also found that the ATH could also induce the crystallization of PLA. The influence of the different fillers and cooling process on the crystalline morphology of PLA is under current investigation.

Conclusions

Polylactide nanocomposites with exfoliated, intercalated MMT structures, and some aggregations in their polymer matrix were successfully prepared via direct melt compounding with ATH and CF using a Brabender. Because the high thermal conductivity of the CF could increase the dissipation rate of heat from the PLA composite, and the incorporation of MMT sheets could form the effective dense layer during burn, and PLA/ATH/MMT/CF nanocomposites with a UL-94 V-0 rating without flame dripping can be obtained via melt compounding. It was found that the tensile strength and elongation at break of the PLA/ATH/MMT nanocomposites could be improved by substituting a portion of the ATH with CF. For example, the breaking strength and elongation of sample F15 (PLA/ATH/MMT/CF weight ratio of 60/20/5/15) are 64.5 MPa and 6.8 %, respectively, which are higher than those of PLA/ATH/MMT nanocomposite without any CF.

Moreover, the sample F15 showed the better flame retardant and anti-dripping properties. The results would be helpful to search for the engineering applications of PLA composites, such as electronic material.

Acknowledgements We thank the National Science Council of Taiwan for their financial support of this study under Contract NSC 101-2221-E-027-024.

References

1. Haafiz MKM, Hassan A, Zakaria Z, Inuwa IM, Islam MS, Jawaid M (2013) Properties of polylactic acid composites reinforced with oil palm biomass microcrystalline cellulose. Carbohydr Polym 98:139–145
2. Ajioka M, Enomoto K, Suzuki K, Yamaguchi A (1995) The basic properties of poly(lactic acid) produced by the direct condensation polymerization of lactic acid. J Environ Polym Degrad 3:225–234
3. Auras R, Harte B, Selke S (2004) An overview of polylactides as packaging materials. Macromol Biosci 4:835–864
4. Fukushima K, Murariu M, Camino G, Dubois P (2010) Effect of expanded graphite/layered-silicate clay on thermal, mechanical and fire retardant properties of poly(lactic acid). Polym Degrad Stab 95:1063–1076
5. Ke C-H, Li J, Fang K-Y, Zhu Q-L, Zhu J, Yan Q, Wang Y-Z (2010) Synergistic effect between a novel hyperbranched charring agent and ammonium polyphosphate on the flame retardant and anti-dripping properties of polylactide. Polym Degrad Stab 95:763–770
6. Kumar M, Mohanty S, Nayak SK, Rahail Parvaiz M (2010) Effect of glycidyl methacrylate (GMA) on the thermal, mechanical and morphological property of biodegradable PLA/PBAT blend and its nanocomposites. Bioresour Technol 101:8406–8415
7. Qian Y, Wei P, Jiang P, Li Z, Yan Y, Ji K (2013) Aluminated mesoporous silica as novel high-effective flame retardant in polylactide. Compos Sci Technol 82:1–7
8. Reti C, Casetta M, Duquesne S, Bourbigot S, Delobel R (2008) Flammability properties of intumescent PLA including starch and lignin. Polym Adv Technol 19:628–635
9. Murariu M, Bonnaud L, Yoann P, Fontaine G, Bourbigot S, Dubois P (2010) New trends in polylactide (PLA)-based materials: "Green" PLA-Calcium sulfate (nano)composites tailored with flame retardant properties. Polym Degrad Stab 95:374–381
10. Tang G, Wang X, Xing W, Zhang P, Wang B, Hong N, Yang W, Hu Y, Song L (2012) Thermal degradation and flame retardance of biobased polylactide composites based on aluminum hypophosphite. Ind Eng Chem Res 51:12009–12016
11. Feijoo JL, Cabedo L, Gimenez E, Lagaron JM, Saura JJ (2005) Development of amorphous PLA-montmorillonite nanocomposites. J Mater Sci 40:1785–1788. doi:10.1007/s10853-005-0694-8
12. Solarski S, Mahjoubi F, Ferreira M et al (2007) Plasticized polylactide/clay nanocomposite textile: thermal, mechanical, shrinkage and fire properties. J Mater Sci 42:5105–5117. doi:10.1007/s10853-006-0911-0
13. Gilman JW (1999) Flammability and thermal stability studies of polymer layered-silicate (clay) nanocomposites. Applied Clay Sci 15:31–49
14. Kiliaris P, Papaspyrides CD, Pfaendner R (2008) Polyamide 6 filled with melamine cyanurate and layered silicates: evaluation of flame retardancy and physical properties. Macromol Mater Eng 293:740–751
15. Wu D, Wu L, Wu L, Zhang M (2006) Rheology and thermal stability of polylactide/clay nanocomposites. Polym Degrad Stab 91:3149–3155
16. Kashiwagi T, Morgan AB, Antonucci JM, Van Landingham MR, Harris RH, Awad WH, Shields JR (2003) Thermal and flammability properties of a silica–poly(methylmethacrylate) nanocomposite. J Appl Polym Sci 89:2072–2078
17. Morgan AB (2006) Flame retarded polymer layered silicate nanocomposites: a review of commercial and open literature systems. Polym Adv Technol 17:206–217
18. Chuang T-H, Guo W, Cheng K-C, Chen S-W, Wang H-T, Yen Y-Y (2004) Thermal properties and flammability of ethylene-vinyl acetate copolymer/montmorillonite/polyethylene nanocomposites with flame retardants. J Polym Res 11:169–174
19. Cheng K-C, Yu C-B, Guo W, Wang S-F, Chuang T-H, Lin Y-H (2012) Thermal properties and flammability of polylactide nanocomposites with aluminum trihydrate and organoclay. Carbohydr Polym 87:1119–1123
20. Wan YZ, Wang YL, Li QY, Dong XH (2001) Influence of surface treatment of carbon fibers on interfacial adhesion strength and mechanical properties of PLA-based composites. J Appl Polym Sci 80:367–376
21. Shen L, Yang H, Ying J, Qiao F, Peng M (2009) Preparation and mechanical properties of carbon fiber reinforced hydroxyapatite/polylactide biocomposites. J Mater Sci 20:2259–2265. doi:10.1007/s10856-009-3785-2
22. Dondero WE, Gorga RE (2006) Morphological and mechanical properties of carbon nanotube/polymer composites via melt compounding. J Polym Sci Part B 44:864–878
23. Wang C, Ying S (2013) Batch foaming of short carbon fiber reinforced polypropylene composites. Fibers Polym 14:815–821
24. Ray SS, Okamoto M (2003) Polymer/layered silicate nanocomposites: a review from preparation to processing. Prog Polym Sci 28:1539–1641
25. Lepoittevin B, Devalckenaere M, Pantoustier N, Alexandre M, Kubies D, Calberg C, Jerome R, Dubois P (2002) Poly(ε-caprolactone)/clay nanocomposites prepared by melt intercalation: mechanical, thermal and rheological properties. Polymer 43:4017–4023
26. Rahatekar SS, Zammarano M, Matko S, Koziol KK, Windle AH, Nyden M, Kashiwagi T, Gilman JW (2010) Effect of carbon nanotubes and montmorillonite on the flammability of epoxy nanocomposites. Polym Degrad Stab 95:870–879
27. Wang M, Kang Q, Pan N (2009) Thermal conductivity enhancement of carbon fiber composites. Appl Therm Eng 29:418–421
28. Zou GX, Zhang X, Zhao CX, Li J (2012) The crystalline and mechanical properties of PLA/layered silicate degradable composites. Polym Sci A 54:393–400